Pharm Res (2010) 27:2753–2765
DOI 10.1007/s11095-010-0277-5

RESEARCH PAPER

Delivery of Water-Soluble Drugs Using Acoustically Triggered Perfluorocarbon Double Emulsions

Mario L. Fabiilli • James A. Lee • Oliver D. Kripfgans • Paul L. Carson • J. Brian Fowlkes

Received: 9 June 2010 / Accepted: 13 September 2010 / Published online: 25 September 2010

ABSTRACT

Purpose Ultrasound can be used to release a therapeutic payload encapsulated within a perfluorocarbon (PFC) emulsion via acoustic droplet vaporization (ADV), a process whereby the PFC phase is vaporized and the agent is released. ADV-generated microbubbles have been previously used to selectively occlude blood vessels *in vivo*. The coupling of ADV-generated drug delivery and occlusion has therapeutically synergistic potentials.

Methods Micron-sized, water-in-PFC-in-water (W_1/PFC/W_2) emulsions were prepared in a two-step process using perfluoropentane (PFP) or perfluorohexane (PFH) as the PFC phase. Fluorescein or thrombin was contained in the W_1 phase.

Results Double emulsions containing fluorescein in the W_1 phase displayed a 5.7±1.4-fold and 8.2±1.3-fold increase in fluorescein mass flux, as measured using a Franz diffusion cell, after ADV for the PFP and PFH emulsions, respectively. Thrombin was stably retained in four out of five double emulsions. For three out of five formulations tested, the clotting time of whole blood decreased, in a statistically significant manner ($p < 0.01$), when incubated with thrombin-loaded emulsions exposed to ultrasound compared to emulsions not exposed to ultrasound.

Conclusions ADV can be used to spatially and temporally control the delivery of water-soluble compounds formulated in PFC double emulsions. Thrombin release could extend the duration of ADV-generated, microbubble occlusions.

KEY WORDS acoustic droplet vaporization · double emulsion · embolization · perfluorocarbon · thrombin · ultrasound · vascular occlusion

ABBREVIATIONS

ACT	activated clotting time
ADV	acoustic droplet vaporization
CPD	citrate-phosphate-dextrose
IU	international units
PEG	polyethylene glycol
PFC	perfluorocarbon
PFH	perfluoro-n-hexane
PFP	perfluoro-n-pentane
PRP	pulse repetition period
US	ultrasound
W_1/PFC/W_2	water-in-perfluorocarbon-in-water

INTRODUCTION

Particles that release a therapeutic payload upon interaction with an internal stimulus, such as pH or hypoxia, or the application of an externally applied stimulus, such as heat or ultrasound (US), are being studied in an effort to localize drug delivery to target areas (1–5). The control of localized delivery is especially important for drugs that possess narrow therapeutic windows, thereby minimizing systemic side effects. US-triggered drug delivery is unique since US affords

M. L. Fabiilli · O. D. Kripfgans · P. L. Carson · J. B. Fowlkes
Department of Biomedical Engineering, University of Michigan
Ann Arbor, Michigan, USA

M. L. Fabiilli · J. A. Lee · O. D. Kripfgans · P. L. Carson · J. B. Fowlkes
Department of Radiology, University of Michigan
Ann Arbor, Michigan, USA

O. D. Kripfgans
Applied Physics Program, University of Michigan
Ann Arbor, Michigan, USA

M. L. Fabiilli (✉)
1301 Catherine Street, 3225 Medical Sciences Building I
Ann Arbor, Michigan 48109-5667, USA
e-mail: mfabiill@umich.edu

diagnostic and therapeutic capabilities, spatial and temporal control of delivery, and the ability to focus onto deeply located tissues. The interaction of US with payload-containing particles can generate acoustic cavitation, heating, radiation forces, and sonoporation. The last effect, the transient increase in cell membrane permeability, can greatly enhance the uptake of drugs, genes, and peptides contained within US-activated particles (6–9). These particle-US interactions can also produce therapeutic effects to be utilized in diverse applications such as thrombolysis (10) or in the reversible disruption of the blood-brain barrier (11).

Colloidal particles utilized in US-mediated drug release are typically shell-stabilized microbubbles or droplets containing, respectively, perfluorocarbon (PFC) gases or liquids. The former colloids evolved from clinically-utilized US contrast agents, which are micron-sized gas bubbles that increase the echogenicity in perfused tissue upon intravenous administration. Due to their size, the microbubbles are transpulmonary and resonant at frequencies utilized in clinical imaging systems (12). Therapeutic agents are typically incorporated into the microbubbles using one of the following methods: attachment to or intercalation within the shell, complexation of secondary carriers to the microbubble shell, or incorporation within a fluid inside the shell (13,14).

As highlighted in a recent review (15), PFC emulsions have also been studied as US contrast agents and drug delivery systems due to their increased stability, longer circulation times, and ability to extravasate if formulated as nanoparticles. Due to the hydrophobicity and lipophobicity of the dispersed PFC phase (16), therapeutic agents are typically loaded into the emulsion using similar techniques as those mentioned for microbubble delivery systems. One commonly utilized method is the use of an oil phase, containing the therapeutic agent, co-emulsified with the PFC phase during formulation (17–20). PFC emulsions, with or without a therapeutic payload, can be vaporized into gas bubbles using US, a mechanism termed acoustic droplet vaporization (ADV) (21–25). ADV is a phenomenon whereby vaporization occurs only if the emulsion is exposed to acoustic amplitudes greater than a threshold value. PFCs used in emulsions suitable for ADV applications typically possess bulk boiling points that are lower than normal body temperature (37°C), such as perfluoropentane (29°C boiling point). Upon injection *in vivo*, the emulsions do not spontaneously vaporize due to the increased internal (i.e. Laplace) pressure, and hence boiling point elevation, of the PFC when formulated as droplets (25). Low-boiling-point PFCs, such as perfluoropentane, also enable the use of lower acoustic amplitudes to generate ADV (17) and the production of stable gas bubbles *in vivo* (26–28). The ADV of PFC emulsions containing a lipophilic, therapeutic payload can be used to facilitate the delivery and release of the therapeutic agent, as demonstrated with *in vitro* (17–20) and *in vivo* (25) studies.

The ADV of micron-sized PFC emulsions, administered intravenously or intraarterially, has also been used to generate localized, vascular occlusion *in vivo* (26–28). The temporal duration of an ADV-generated occlusion is transient, especially for gas emboli generated from intravenously administered emulsions (28). Therefore, the ability to extend this duration may be therapeutically beneficial for surgical applications that require longer occlusion times, such as radiofrequency ablation (29) and high intensity focused US thermal therapy (30). ADV-generated occlusion could also be potentially used to treat hemorrhaging associated with vascular damage or other internal bleeding, which are currently treated using transcatheter embolization (31,32). One option is the simultaneous formation of a chemically generated embolus and gas embolus within the feeder artery of the target tissue, thereby prolonging the duration of ADV-generated embolization. Chemical embolic agents, such as N-butyl cyanoacrylate, ethylene vinyl alcohol copolymer, and Eudragit E-100 (used in the treatment of arteriovenous malformations (33–35)) or thrombin (used in the treatment of pseudoaneurysms (36,37)), are typically administered via the use of a catheter. Therefore, the encapsulation of a chemical embolic agent within a PFC emulsion could provide a minimally invasive means of producing a localized, sustained embolization via ADV with millimeter precision and without the use of ionizing fluoroscopy.

The aim of this study was to develop a PFC emulsion containing a water-soluble, chemical embolic agent, thereby expanding the range of therapeutic agents delivered via ADV beyond oil-soluble compounds. The micron-sized PFC emulsions were formulated as double emulsions with the following structure: water-in-PFC-in-water (W_1/PFC/W_2). These double emulsions can serve as a prototype carrier for other water-soluble therapeutic agents. In the first section, PFC double emulsions containing fluorescein—a hydrophilic fluorophore—are prepared and studied to demonstrate the proof-of-concept that fluorescein encapsulation within a PFC double emulsion delays its release until US exposure. The ability of ADV to release the encapsulated fluorescein is also evaluated. In the second section, the encapsulation of a chemical embolic agent, thrombin (factor IIa)—a serine protease in the coagulation cascade that converts fibrinogen into fibrin—is explored using different emulsification techniques. The effects of the various techniques are studied in terms of the resulting emulsion, with a focus on thrombin stability and retention. ADV of the thrombin-loaded emulsion is achieved using ultrasound parameters suitable for *in vivo* applications.

MATERIALS AND METHODS

Fluorosurfactant Synthesis

The copolymer used to stabilize the primary emulsion (W_1/PFC) was synthesized using a two-step process, as seen in Fig. 1 and outlined in Holtze *et al.* (38). First, Krytox 157 FSL (DuPont, Wilmington, DE, USA)—a perfluoroether with carboxylic acid functionality—was converted to an acid chloride using methods previously described (39,40). Briefly, under a nitrogen purge, Krytox 157 FSL was added to a round-bottom flask containing HFE-7100 (3M, St. Paul, MN, USA), a mixture of methyl nonafluoroisobutyl ether and methyl nonafluorobutyl ether. Thionyl chloride (Sigma Aldrich, St. Louis, MO, USA) was then added in a 10:1 molar excess relative to the Krytox 157 FSL. The flask was refluxed with a condenser and stirred for 24 h at 50°C while under a nitrogen purge. The resulting mixture was concentrated using a rotary evaporator. Second, the acid chloride was reacted with polyoxyethylene (PEG) diamine (Sigma Aldrich) to form a copolymer, analogous to previously described methods (39,40). The solvent was a 5:3 volumetric ratio of HFE-7100 and benzotrifluoride (Alfa Aesar, Ward Hill, MA, USA). Similar experimental conditions were used as in the first reaction step. The resulting copolymer, termed Krytox-PEG copolymer, was concentrated using a rotary evaporator, and its structure was confirmed using ^{1}H, ^{13}C, and ^{19}F NMR spectroscopy.

Fluorescein Emulsion Preparation

The primary emulsion was formed by first dissolving, in a 1.5 mL microcentrifuge tube (Thermo Fisher Scientific, Waltham, MA, USA), Krytox-PEG copolymer (6 mg/mL PFC) in 400 μL of either pefluoro-n-pentane (PFP, Alfa Aesar) or perfluoro-n-hexane (PFH, Alfa Aesar). Next, 200 μL of a 100 mg/mL solution of fluoroscein sodium salt (Sigma Aldrich) in normal saline (0.9% w/v, Hospira Inc., Lake Forest, IL, USA) was added to the PFC phase. The mixture was emulsified, while in an ice bath, via sonication using a microtip (Model 450, 20 kHz, 3.2 mm diameter, Branson, Danbury, CT, USA) operating at 125 W/cm^2 for 30 s in continuous mode. In a 2 mL glass vial (Shamrock Glass, Seaford, DE, USA), 250 μL of primary emulsion was then added to 750 μL of a 10 mg/mL solution of Pluronic F-68 (Poloxamer 188, Sigma Aldrich) dissolved in normal saline. The vial was sealed with a rubber stopper and metal cap and subsequently shaken for 45 s at 4,550 cycles per minute using an amalgamator (VialMix, Lantheus Medical Imaging, Billerica, MA, USA). The resulting double emulsion was used immediately after processing, though it was confirmed that the emulsion was stable, in terms of encapsulation efficiency and droplet size distribution, for at least 24 h if stored at 5°C. Table I summarizes the fluorescein emulsions and associated processing parameters.

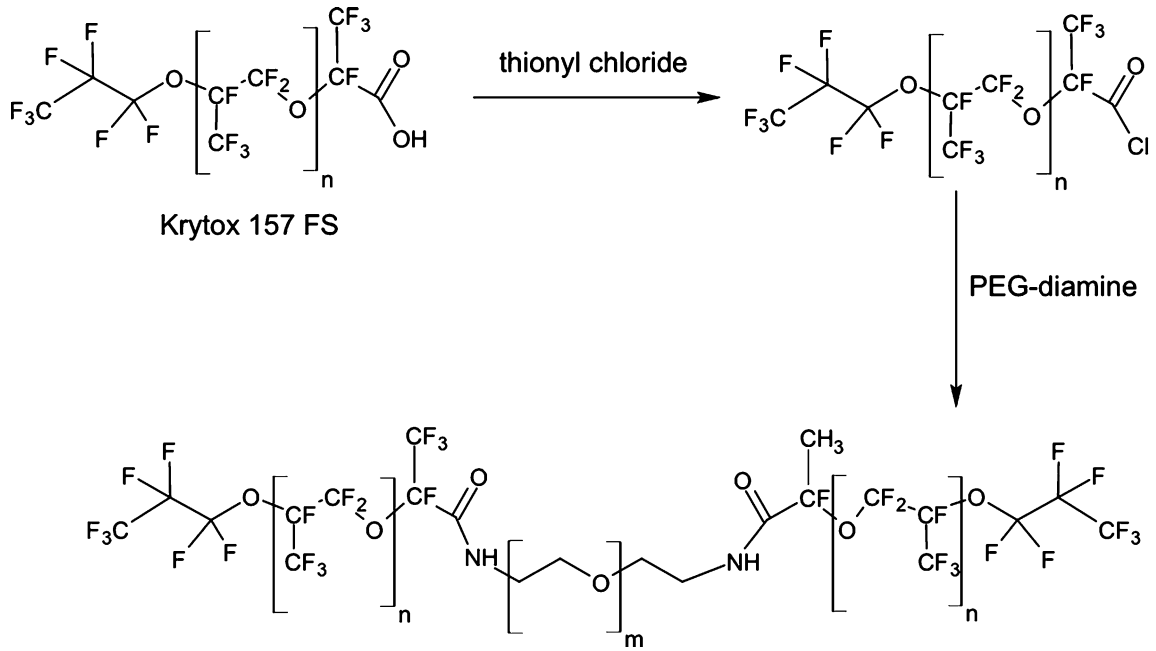

Fig. 1 The Kytox 157L FS is first converted into an acid chloride and then reacted with PEG-diamine to form a copolymer via amide linkages.

Table I Summary of Fluorescein and Thrombin Emulsions Used for Studies. In All Cases, the Primary Emulsion was Formed Using Sonication

Formulation	Compound	PFC	Processing during 2nd emulsification step
F1	Fluorescein	PFP	Shaking
F2	Fluorescein	PFH	Shaking
T1	Thrombin	PFP	Sonication
T2	Thrombin	PFP	Shaking
T3	Thrombin	PFP	Stirring
T4	Thrombin	PFP	Stirring+glass beads
T5	Thrombin (+ xanthan gum)	PFP	Stirring+glass beads

Thrombin Emulsion Preparation

Thrombin (Thrombin-JMI, bovine-origin, King Pharmaceuticals, Bristol, TN, USA) was dissolved in normal saline at a concentration of 5,000 international units (IU) per mL. In a microcentrifuge tube, 300 μL of thrombin solution was combined with 650 μL of PFP, which already contained dissolved Krytox-PEG copolymer (6 mg/mL PFC). The mixure was then sonicated, as previously described for the fluorescein emulsions, to form the primary emulsion. The primary emulsion (475 μL) was combined with a 10 mg/mL solution of Pluronic F-68 in saline (1,200 μL) and emulsified to form the double emulsion. Three processing techniques were explored for the second emulsification step: sonication, shaking, or magnetic stirring. For emulsification via sonication, the primary emulsion was added to a microcentrifuge tube along with the Pluronic F-68 solution and then sonicated as previously described. For emulsification via shaking, the primary emulsion and Pluronic F-68 solution were added to a 2 mL glass vial and processed similarly to the second emulsification step of the fluorescein emulsions. For emulsification via magnetic stirring, the primary emulsion was added to the Pluronic F-68 solution, contained in a 2 mL glass vial, while being stirred at 1,100 rpm for 15 min. The vial was placed in an ice bath during the stirring process. Borosilicate glass balls (2 mm diameter, Chemglass Inc., Vineland, NJ, USA) were added in two formulations (T4 and T5) to reduce the droplet size during the stirring step. Xanthan gum (Sigma Aldrich) was dissolved in the thrombin solution (10 mg/mL) in one formulation (T5) in order to increase the viscosity of the encapsulated aqueous phase; this was done in an effort to decrease the mobility of the thrombin in the W_1 phase and hence the diffusion rate of thrombin from the emulsion (41). All experiments were conducted with emulsions that had been processed immediately prior to use, though it was confirmed that the emulsions were stable, in terms of encapsulation efficiencies and droplet size distributions, for at least 24 h if stored at 5°C. Table I summarizes the various thrombin formulations that were investigated.

Physical Characterization of Emulsions

The structures of the double emulsions containing fluorescein were determined using visible and fluorescent microscopy. Visible micrographs of the thrombin emulsions were also taken. The emulsions were diluted in normal saline, and images were taken using a microscope (Leica DMRB, Bannockburn, IL, USA) and camera (Spot FLEX, Diagnostic Instruments Inc., Sterling Heights, MI, USA), controlled by Spot Advanced software (Diagnostic Instruments Inc.). The emulsions were sized using a Coulter counter (Multisizer 3, Beckman Coulter Inc., Fullteron, CA, USA). Prior to sizing, the emulsions were diluted in normal saline that had been filtered through a 0.22 μm filter (GSWP, Millipore, Billerica, MA, USA). All formulations were sized using a 50 μm aperture, which can count particles between 1.0 and 30 μm. The T3 formulation was also sized with a 140 μm aperture, which can count particles between 2.8 and 84 μm, due to the presence of larger droplets.

Encapsulation Efficiency of Fluorescein Emulsions

The fluorescein emulsions were washed in triplicate to remove unencapsulated fluorescein. Due to the densities of PFP (1.6 g/mL) and PFH (1.7 g/mL), the washing was accomplished by centrifuging the droplets at 1,200 rpm for 3 min. Repeated centrifugation did not cause significant droplet breaking, which was confirmed by measuring the fluorescein concentration in the supernatant after the second and third washings. The concentration of encapsulated fluorescein was determined by adding an aliquot of the washed emulsion to methanol (CHROMASOLV Plus for HPLC, Sigma Aldrich), thereby breaking the emulsion. The fluorescein concentration was determined via fluorescence spectroscopy (LS-50B, PerkinElmer, Waltham, MA, USA) with excitation and emission wavelengths of 485 nm and 525 nm, respectively. The encapsulation efficiency was calculated as the ratio of encapsulated fluorescein to the initial amount of fluorescein loaded into the emulsion (i.e. prior to washing).

In Vitro Fluorescein Release

Fluorescein release from the PFP and PFH emulsions was measured using a Franz diffusion cell (PermeGear, Inc., Hellertown, PA, USA). A cellulose membrane (6–8 kDa molecular weight cutoff, Spectrum Laboratories, Inc., Rancho Dominguez, CA, USA), soaked in normal saline 30 min prior to use, was mounted between the donor and receptor compartments. By comparison, the molecular weight of the ionized form of fluorescein is 328.3 Da. The donor media consisted of 2 mL of fluorescein emulsion, washed in triplicate to remove unencapsulated fluorescein. The receptor media consisted of 7.5 mL of normal saline. Near sink conditions were maintained in the receptor compartment throughout the experiment, with the fluorescein concentration in the receptor compartment never exceeding 0.01% of saturation. The diffusion area between both compartments was 1.77 cm^2. The stirring rate and temperature in the receptor compartment were kept at 600 rpm and 37°C, respectively. Note that for F1, the temperature inside the receptor is above the boiling point of PFP, whereas for F2, the receptor is below the boiling point of PFH. In order to prevent settling of the emulsion onto the membrane, due to the densities of PFP and PFH, an overhead stirrer operating at 600 rpm was used in the donor compartment. At 15-min intervals, aliquots of the receptor medium were withdrawn and immediately replaced with an equal volume of fresh, normal saline. The amount of fluorescein released was determined via fluorescence spectroscopy as previously described.

To determine the effect of ADV on fluorescein release, the PFP and PFH emulsions were placed in 15 mL centrifuge tubes (Thermo Fisher Scientific) and immersed in a water bath heated to 37°C and 64°C, respectively. In each case, the emulsion was warmed to 8°C of superheat, since the normal boiling points of PFP and PFH are 29°C and 56°C, respectively. The emulsions were continuously sonicated for 2 min using the microtip operating at 20 kHz and 312 W/cm^2 in order to generate ADV. Low frequency, continuous wave US, which is difficult to focus *in vivo*, was used to generate ADV—compared to previous studies which used higher frequency (1–10 MHz) pulsed US (17,23,26,27,42,43)—to maximize the cavitation-assisted vaporization of the emulsion during these proof-of-concept studies. The resulting mixture (post-sonication) was then added to the donor compartment of the diffusion cell, and the fluorescein release was determined as previously described. The fluorescein release rates from the emulsion studies were compared to mass fluxes obtained when an equal concentration of fluorescein solution was loaded into the donor compartment. The volume fraction of droplets vaporized after ADV was determined by counting the droplets remaining in the tube post US exposure *versus* a control case (i.e. without US) with a Coulter counter (17). The droplet sample was briefly over-pressurized in a gas-tight syringe in order to destroy existing microbubbles and decrease the likelihood of counting these as droplets.

Encapsulation Efficiency and Stability of Thrombin Emulsions

The encapsulation efficiency of the thrombin double emulsions, immediately following the second emulsification step, was determined by separating the droplets from the continuous, aqueous phase via repeated centrifugation using similar methods as for the fluorescein emulsions. Minimal droplet breakage, assessed as previously described for the fluorescein emulsions, occurred during the washing steps. The non-encapsulated thrombin concentration was estimated using the Pierce 660 nm protein assay (Thermo Fisher Scientific), and the encapsulation efficiency was determined as previously described. The stability of the thrombin encapsulation in the emulsions was determined by heating the emulsion to 37°C while stirring at 1,100 rpm. At 15-min intervals, aliquots were removed and centrifuged to separate the droplets from the continuous phase, and the non-encapsulated thrombin concentration was estimated as previously stated.

In Vitro Thrombin Release

Thrombin release from the emulsions, in blood, was assessed using a modified activated clotting time (ACT) assay. Fresh, whole canine blood was acquired and immediately mixed with citrate-phosphate-dextrose (CPD) solution (Sigma Aldrich), an anticoagulant, in a volumetric ratio of 10:1.4, respectively. CPD, used in the storage of whole blood, prevents coagulation via the chelation of calcium ions with citrate (44). The blood was stored at 4°C and used within 7 days of acquisition. All protocols involved in the blood acquisition were approved by the University of Michigan Committee on the Use and Care of Animals (UCUCA).

The effect of thrombin concentration on the ACT was determined as follows. First, 0.4 mL of blood containing CPD was added to a plastic, ACT test tube (International Technidyne Corporation, Edison, NJ, USA), which contained approximately 30 mg of glass beads (119.6 μm mean diameter) and a magnet. Then, an aliquot of thrombin solution was added to the tube. The volume of thrombin added never exceeded 50 μL. Finally, the tube was capped, gently mixed, and placed into the Hemochron 400 (International Technidyne Corporation). The instrument mechanically detected the formation of a fibrin clot via the rotation of the magnet within the tube. Upon

clotting, the magnet lifted within the tube; the time for this to occur was the ACT. Due to the possibility of thrombin denaturation or loss of activity during the emulsion processing, thrombin solutions were subjected to identical processing conditions, as seen in Table I. These solutions were tested for thrombin activity using the ACT assay. Additionally, due to the antithrombotic properties of Pluronic F-68 (45,46), each emulsion component—Pluronic F-68, PFP, and Krytox-PEG copolymer—and the blank emulsion (i.e. without thrombin) were combined with a known concentration of thrombin to determine its effect on the ACT. The ACT was measured with each thrombin emulsion as well.

To determine the effect of ADV on thrombin release, each emulsion was injected into an OptiCell™ (Thermo Fisher Scientific) chamber and exposed to US using a previously utilized experimental setup (17). The chamber was placed into an OptiCell™ holder that was located within a tank (40×60×27 cm) containing degassed, deionized water heated to 37°C. The surface of the tank water was covered with air-filled plastic balls (Cole-Parmer Inc., Vernon Hills, IL, USA) to minimize regassing and heat loss as well as scattering the reflected US at the air/water surface. A calibrated 3.5 MHz single-element transducer (1.9 cm diameter, 3.81 cm focal length, A381S, Panametrics, Olympus NDT Inc., Waltham, MA) was positioned below the chamber and focused on the bottom window of the chamber. Acoustic pulses generated by the transducer—3.7 μs pulse duration, 10 ms pulse repetition period (PRP), 4.7 MPa peak rarefactional pressure, 11.3 MPa peak compressional pressure—were achieved using a function generator (33120A, Agilent Technologies, Palo Alto, CA, USA) and power amplifier (55 dB, model A-300, E & I, Rochester, NY, USA). The transducer was rastered via a computer-controlled positioning system at 4 mm/s across the chamber surface in order to vaporize the emulsion. Due to the volume of emulsion introduced into the OptiCell™(1 mL), only a fraction of the chamber surface was covered by the emulsion and subsequently insonified. The raster spacing was 0.5 mm; by comparison, the −6 dB lateral beam width of the transducer was 0.88 mm. The total exposure time was 5 min. Following the US exposure, the mixture was removed from the OptiCell™, and the ACT was measured as described previously. The volume fraction of droplets vaporized was determined by counting the droplets remaining in the OptiCell™ post US exposure *versus* a control case (i.e. without US) with the Coulter counter, as described previously for the fluorescein emulsions.

Statistical Analysis

Each experimental value is expressed as mean±standard deviation and the result of at least three independent measurements. Statistically significant differences between experimental groups were determined using a Student's *t*-test. A significance level of 0.01 was used for all comparisons.

RESULTS

Physiochemical Characterization of Fluorescein Emulsions

Representative micrographs of the fluorescein emulsions are displayed in Fig. 2. The aqueous droplets containing fluorescein (W_1), stabilized by the Krytox-PEG copolymer, are surrounded by PFC. The fluorescein droplets comprise a large volume fraction and are homogenously distributed within the PFC globule. Similar structures were observed for the thrombin emulsions. As seen in Table II, the mean diameter of fluorescein emulsions containing PFP and PFH—F1 and F2, respectively—were not statistically different. Additionally, the encapsulation efficiencies for F1 and F2 were not statistically different either.

In Vitro Release of Fluorescein

The retention of fluorescein within the emulsions, as evaluated using a Franz diffusion cell, is shown in Fig. 3. The values in Fig. 3 were corrected for the aliquots of

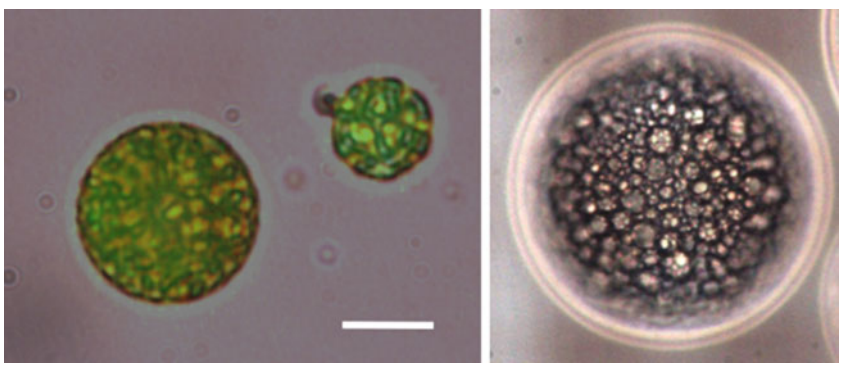

Fig. 2 Micrographs of a W_1/PFC/W_2 emulsion containing fluorescein in the W_1 phase. The left image is an overlay of both visible and fluorescent micrographs. The scale bar is 8 μm. The structure of the W_1/PFC/W_2 emulsion—water droplets containing fluorescein within a globule of PFC—can be clearly seen in the right image, which displays a 100 μm diameter globule.

Table II Characterization of Fluorescein and Thrombin Emulsions. Thrombin Precipitation, During the Second Emulsification Step, and Subsequent Inactivation of Thrombin During ADV was Suspected in T2

Formulation	Mean diameter (μm)	Percent of droplets >6 μm diameter		Encapsulation (%)	Volume percent vaporized	Percent change in ACT upon ADV
		Number	Volume			
F1	2.5±0.1	4.3±1.3	53.1±9.4	5.4±1.0	100 [c]	NA
F2	2.4±0.2	2.6±1.8	32.3±15.4	3.8±1.1	100 [c]	NA
T1	1.6±0.1	0.04±0.02	6.7 ±3.0	76.3±3.4	10.2±4.2	−7.4±1.6
T2	2.6±0.2	6.5±1.4	83.2±1.0	63.7±22.9 [a]	25.6±7.1	63.0±12.2 [a,b]
T3	27.4±5.9	89.2±1.1	99.9±0.1	97.5±0.6	100 [c]	−78.0±13.5 [b]
T4	3.5±0.1	15.5±0.8	89.4±4.5	98.8±1.1	28.7±10.2	−23.3±5.9 [b]
T5	3.9±0.1	17.6±0.5	88.9±3.1	97.2±0.5	34.3±15.9	−19.0±4.9 [b]

[a] T2 parameters that are potentially affected by thrombin precipitation; [b] Statistically significant differences for the percent change in ACT upon ADV; [c] Cases where complete vaporization was observed, and thus the number of droplets remaining in solution after ADV was below the noise threshold of the Coulter counter

solution and, hence, fluorescein mass removed during sampling. An aqueous solution of fluorescein, equal in concentration to each emulsion, was used as a control. It was confirmed, by mixing blank emulsion (i.e. without fluorescein) and fluorescein solution, that the presence of droplets within the donor compartment did not statistically change the fluorescein diffusion across the membrane for the fluorescein in solution. Therefore, the encapsulation of fluorescein within the emulsion delayed its release, as is evident in Fig. 3, relative to the fluorescein solution.

The fluorescein flux was calculated based on a linear regression of the data between 15 and 60 min, which yielded squared correlation coefficients (r^2) greater than 0.95 in all cases. The fluxes for F1 and F2 were 0.19±0.02 μg/cm^2/min and 0.07±0.01 μg/cm^2/min, respectively. Note that the concentration of encapsulated fluorecein in F1 is higher than F2, 0.6 mg/mL *versus* 0.3 mg/mL. By comparison, when F1 and F2 are exposed to US and fluorescein is released via ADV, the fluxes increase to 1.12±0.24 μg/cm^2/min and 0.60±0.04 μg/cm^2/min, respectively. This corresponds to a 5.7±1.4- and 8.2±1.3-fold increase in flux for F1 and F2, respectively. These fluxes are not statistically different from the fluxes obtained for fluorescein solutions of equal concentration. This is expected, considering that all of the droplets had been vaporized as a result of ADV, as seen in Table II.

Physiochemical Characterization of Thrombin Emulsions

Table II lists the mean diameters for the five different thrombin emulsions (T1-T5). The percent of droplets greater than 6 μm diameter, in terms of both number and volume, are included to indicate how suitable the emulsions are for intravenous administration. The percent of thrombin encapsulation is also included in Table II. T1, processed via sonication during the second emulsification step, yielded the smallest mean diameter (1.6 μm). The

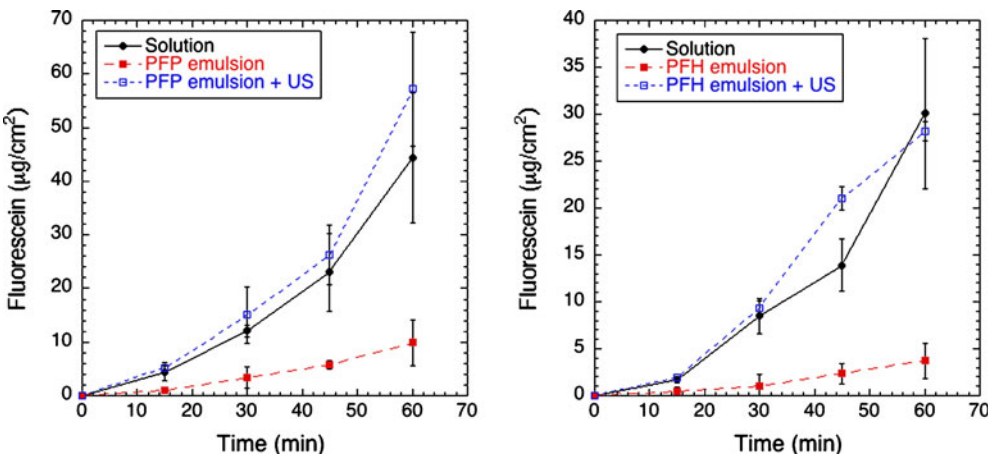

Fig. 3 *In vitro* release profiles of PFP (*left*) and PFH (*right*) double emulsions containing fluorescein at 37°C. In each case, the release profiles obtained from the emulsion, with and without ADV, are compared to a solution of fluorescein of equal concentration. The fluorescein concentration for the PFP and PFH emulsions are 0.6 mg/mL and 0.3 mg/mL, respectively.

shaken formulation, T2, yielded a mean diameter (2.6 μm) that was not statistically different from the similarly processed fluorescein emulsions (F1 and F2). Alternatively, T3—processed via stirring—yielded the largest mean diameter (27.4 μm). The addition of glass beads, in an effort to increase the shear force generated during stirring, caused the mean diameters of T4 and T5 to decrease to 3.5 μm and 3.9 μm, respectively.

The thrombin emulsions were initially loaded with a thrombin concentration of 417 IU/mL. The largest encapsulation efficiencies were obtained for the emulsions that were stirred in the second emulsification step (T3-T5). The second emulsification step is critical when forming double emulsions, since excess shear or mixing can cause the W_1 phase of the primary emulsion (i.e. W_1/PFC) to coalesce with the external aqueous phase (i.e. W_2) (47). Therefore, emulsification techniques that generate lower shear forces, such as stirring, are amenable in the second emulsification step (48). Pair-wise comparisons between T3, T4, and T5 indicate no statistically significant differences in the encapsulation efficiencies. Thus, in the case of T4, the addition of glass beads decreased the droplet size without compromising thrombin encapsulation. Additionally, increasing the viscosity of the W_1 phase more than 1000-fold (49), as in T5, did not affect the encapsulation efficiency. As will be discussed in the next section, the encapsulation efficiency of T2 is skewed by the denaturation of thrombin during the second emulsification step. Upon warming the thrombin emulsions to 37°C and stirring simultaneously, no statistically significant changes were observed in the encapsulation efficiency over a 1-h period for any of the thrombin emulsions.

Formulation Parameters Affecting Thrombin Activity

Figure 4 displays the measured ACT for different thrombin levels. The data was fit ($r^2 > 0.94$) using a sigmoidal curve utilized in previous works (17,42). There were no statistically significant differences with the ACT data between 2.4 IU/mL and 24 IU/mL. Due to the susceptibility of proteins to aggregate, denature, or lose activity during encapsulation processes (50), the thrombin activity was measured—in terms of ACT—for thrombin solutions that had been subjected to sonication, shaking, or stirring. No statistically significant differences were observed in ACT, compared to the data in Fig. 4, when the thrombin solution was sonicated, shaken, or stirred. For the sonicated and stirred cases, the thrombin solution was placed in an ice bath during the processing, and no significant temperature increase was measured throughout the processing. For the shaken case, the thrombin solution was chilled to 0°C prior to shaking; the temperature of the thrombin solution inside the sealed vial, measured using a needle-type thermocouple inserted through the rubber stopper, was 30°C after shaking. By comparison, human thrombin begins to denature above 45°C (51). Processing the thrombin solution twice, as seen in Table I for T1-T5, yielded no statistically significant differences, relative to Fig. 4, except in the case of T2 (i.e. sonication followed by shaking), where an approximate 300% increase in ACT was observed. This increase in ACT was attributed to thrombin precipitation, as confirmed visually and also with the colorimetric protein assay. Interestingly, switching the processing order (i.e. shaking followed by sonication) did not cause a statistically significant difference in the ACT.

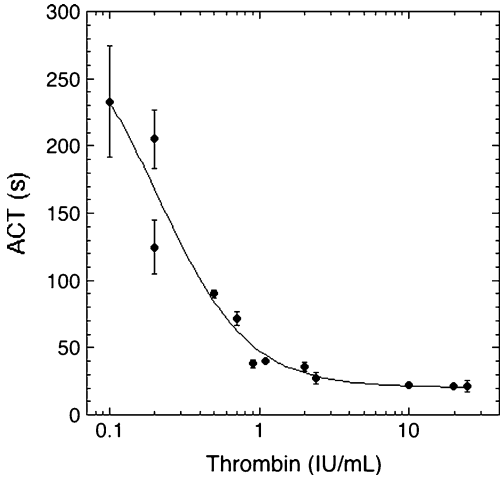

Fig. 4 Reference curve displaying the activated clotting time (ACT) for canine blood, stored with citrate-phosphate-dextrose (CPD) solution, as a function of thrombin concentration.

Each emulsion component—Krytox-PEG copolymer, PFP, and Pluronic F-68—along with the blank emulsion was combined with a known concentration of thrombin (in solution) to determine its effect on the ACT. The addition of PFP, up to 1000x greater in concentration relative to the emulsions, did not cause a statistically significant difference in the ACT. Pluronic F-68, a polymer with known antithrombotic properties (45,46) even in the presence of weak coagulation agonists, did not produce a statistically significant difference in the ACT when added at concentrations up to 100 mg/mL, which is 10x greater than the concentration used for the emulsions. This is likely due to the use of thrombin, which is a strong coagulation agonist, to form clots. As seen in Fig. 5, blank emulsions produced with increasing levels of Krytox-PEG copolymer did produce a statistically significant increase in the ACT. The introduction of low concentrations of copolymer (i.e. $\leq$ 0.018 mg/mL blood) did not significantly change the ACT, but a very large change (i.e. > 1,100% increase) was observed at higher Krytox-PEG copolymer concentrations (i.e. $\geq$ 0.05 mg/mL blood). No statistically significant differences were observed in mean droplet diameter or

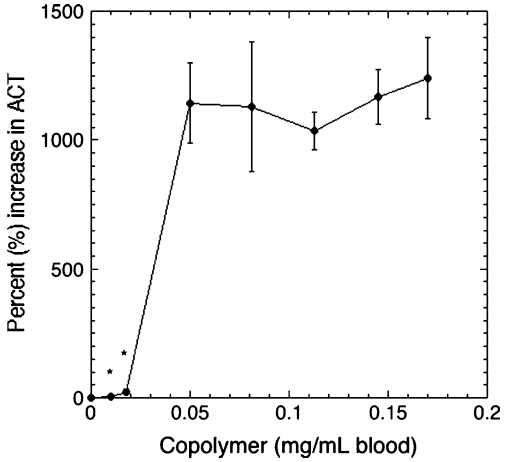

Fig. 5 Anticoagulative effect of the Krytox-PEG copolymer used in the thrombin emulsions. A blank emulsion containing Krytox-PEG copolymer was mixed with thrombin solution. An aliquot of the resulting mixture, containing 1 IU of thrombin, was added to blood containing CPD. Points marked with an asterisk (*) indicate copolymer levels that are not statistically different than the control case (i.e. without copolymer).

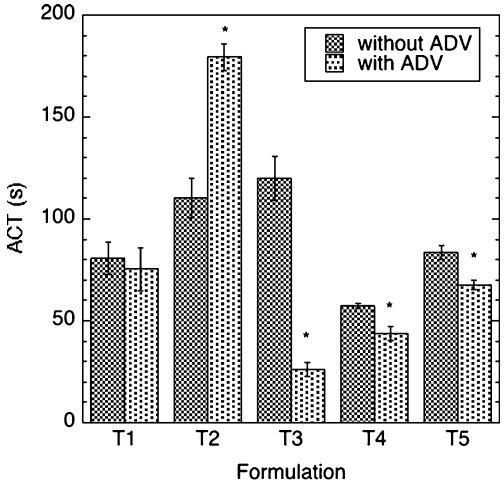

Fig. 6 The effect of ADV (3.5 MHz, 3.7 μs pulse duration, 10 ms PRP, 4.7 MPa peak rarefactional pressure, 11.3 MPa peak compressional pressure, 5 min exposure) on the ACT for five different thrombin formulations. Cases where the ACT was statistically different after ADV are denoted by an asterisk (*).

droplet number density (i.e. number of droplets per mL emulsion) across the range of tested Krytox-PEG copolymer concentrations. Therefore, the thrombin emulsions used for subsequent experiments, including for the data generated in Table II, were formulated using low concentrations of Krytox-PEG copolymer.

In Vitro Release of Thrombin

The validation of ADV-triggered release of thrombin from double emulsions was determined using the ACT assay. As an indicator of thrombin retention within the emulsion, the goal was to maximize and minimize the ACT without and with ADV, respectively. Conceptually, the former goal translates into an infinite ACT for the case where thrombin is highly retained in the emulsion, due to the presence of CPD in the blood. The latter goal, as seen in Fig. 4, corresponds to an ACT of approximately 22 seconds. Fig. 6 displays the ACT obtained for each thrombin emulsion listed in Table II with and without ADV. For four out of five formulations, T1 and T3-T5, a decrease in ACT was observed when the emulsion was exposed to US, compared to the case without US; three out five formulations (T3-T5) exhibited decreases that were statistically significant. Upon US exposure, T2 displayed an increase in ACT compared to the case without US. The largest and smallest ACTs, prior to US exposure, were exhibited by T3 and T4, respectively. T3 displayed the smallest ACT and largest absolute percent change in ACT after ADV. A higher ACT (without ADV case) was observed for T5 (with xanthan gum) relative to T4 (without xanthan gum), though the percent change in ACT upon ADV was not statistically different for T4 and T5. Additionally, as indicated in Table II, the droplets in T2 were completely vaporized after ADV. Table III shows the thrombin concentration in blood, with and without ADV, calculated using the sigmoidal fit in Fig. 4 and the ACT values in Fig. 6. The values in Table III are smaller than the theoretical thrombin concentration (46.3 IU/mL), assuming the complete release of thrombin from the emulsion and no inactivation.

DISCUSSION

This study focuses on the development of PFC double emulsions that carry a water-soluble payload and release the payload upon ADV. In general, the coupling of drug release with ADV has three potential therapeutic advantages, beyond the advantages previously described for US-triggered drug delivery; these synergisms are unique to therapies involving ADV and build upon previous studies involving ADV-induced vascular occlusion (26–28). First,

Table III The Thrombin Concentration in Blood, Estimated from the Regression in Fig. 4 and the Data from Fig. 6. The Thrombin Concentration, Assuming the Complete Release of Thrombin from the Emulsion and No Inactivation, Should have been 46.3 IU/mL

	Thrombin concentration (IU/mL blood)	
Formulation	Without ADV	With ADV
T1	0.5 ± 0.05	0.6 ± 0.09
T2	0.4 ± 0.03	0.2 ± 0.01
T3	0.3 ± 0.03	3.1 ± 0.4
T4	0.8 ± 0.01	1.1 ± 0.7
T5	0.5 ± 0.02	0.6 ± 0.02

the simultaneous release of a chemical embolic agent, such as thrombin, upon ADV can be used to sustain an ADV-generated microbubble embolization. Second, the ischemia generated by vascular occlusion could increase the residence time of a therapeutic agent within the occluded tissue region, potentially increasing the amount of agent that diffuses into the tissue. Third, prolonged ischemia can generate hypoxia, which could be used to activate water-soluble, bioreductive prodrugs, such as NLCQ-1 (52), encapsulated within the emulsion.

Due to the extremely hydrophobic and lipophobic qualities of PFCs (16), the choice of surfactants suitable for stabilizing reverse PFC emulsions (i.e. W/PFC) is quite limited (38,53). The synthesized Krytox-PEG copolymer enabled the formation of a stable primary emulsion (W_1/PFC) compared to primary emulsions prepared using the unmodified Krytox. This is likely due to the presence of the hydrophilic PEG group that stabilizes the W_1/PFC interface (54). The use of a non-ionic hydrophilic group minimizes potential interactions between the surfactant and charged therapeutic agents, such as proteins, which could lose biological activity while encapsulated in the W_1 phase (55). Similarly structured Krytox-PEG copolymers have displayed favorable biocompatibility properties when used to encapsulate mammalian cells or small multicellular organisms within aqueous microcompartments surrounded by PFC (38,56).

The PFC layer separating the payload containing W_1 phase from the exterior W_2 phase serves a dual purpose. First, the PFC acts as a diffusion barrier, thereby preventing the inward or outward diffusion of material, such as the payload, from the W_1 phase; this is clearly seen, for example, in Fig. 3 and with the calculated fluxes for F1 and F2. The minimization of payload diffusion from the emulsion is important in order to couple payload release with ADV of the emulsion. Since the viscosities of PFP (0.64 mPa·s) and PFH (1.11 mPa·s) are close to that of saline (i.e. W_1 phase), the barrier property of the PFC phase is likely attributed to the hydrophobic and lipophobic properties of the PFC (16) and not caused by any restriction in payload diffusion due to the PFC viscosity (41). Second, the PFC phase vaporizes upon ADV, thereby releasing the W_1 phase into the W_2 phase. Since the ADV threshold scales inversely with degree of PFC superheat when the degree of superheat is negative (42), low-boiling-point liquids should be used as the vaporizable phase of the emulsion in order to minimize the acoustic energy required for ADV to occur at normal body temperature. Straight-chain PFCs, such as PFP, meet this boiling point requirement along with being biocompatible and inert (16). Previous studies with PFC droplets (42) and PFC droplets containing an oil layer (18,19) demonstrated an increase in mean droplet size as the boiling point, and hence viscosity, of the PFC phase increased. An increase in the dispersed phase viscosity is known to cause an increase in particle size (57). Since F1 and F2—composed of PFP and PFH, respectively—possessed mean diameters that were not statistically different, this may imply that the volume fraction of PFC within each globule is relatively small such that the globule viscosities of F1 and F2 are similar.

Currently, the primary clinical use of thrombin is topical hemostasis (58). The intravascular use of thrombin has been limited to procedures where thrombin is administered via a catheter, as in the treatment of pseudoaneurysms (36,37), due to the risk of mortality associated with extensive intravascular clotting. The encapsulation of thrombin within a PFC emulsion and its subsequent release upon ADV could enable the targeted formation of thrombi within the vasculature. Additionally, due to the short (<15 s) half-life of thrombin in human plasma (59), a colloidal thrombin formulation could increase the stability of the administered thrombin (60–62).

Thrombin activity, as measured via the ACT assay, was maintained during all emulsification steps except in the case of T2 (sonication followed by shaking). Structural changes, denaturation, and loss of activity can occur when proteins are exposed to US (63) or high shear rates (64). Thus, sonication (under chilled conditions) may have rendered the thrombin more susceptible to denaturation during shaking, where a temperature increase and high shear stresses were generated. Interestingly, the reverse processing conditions were not harsh enough to reduce the thrombin activity. In addition, thrombin activity was impacted by the presence of high levels of the synthesized, Krytox-PEG copolymer (Fig. 5). In this study, Pluronic F-68, a polymer with known antithrombotic properties (45,46), did not alter the ACT in the presence of thrombin. Pluronic F-68 can become embedded into the cell membrane of platelets, thereby inhibiting platelet aggregation by sterically hindering interactions between platelets and lowering interfacial tension (45). Due to the structural similarities between the Krytox-PEG copolymer and Pluronic F-68, it is possible that the mechanism causing an inhibition in platelet aggregation is similar in both cases. When the emulsions with high Krytox-PEG copolymer concentrations were washed in triplicate (via centrifugation), the obtained ACTs were not statistically different from the control case. This observation, combined with the statistically constant droplet diameter and number density across the range of Krytox-PEG copolymers tested, suggest that excess copolymer was present when the concentration exceeded 0.05 mg/mL blood.

The thrombin emulsions displayed higher percent encapsulations than the fluorescein emulsions. This may be due to the smaller osmotic pressure difference across the

W_1/W_2 phases of the thrombin emulsion. Large differences in osmotic pressure can cause the rapid breakdown of double emulsions to simple emulsions (i.e. PFC/W) (65). Despite the stable retention of thrombin within the emulsions over a 1-h period, some thrombin was released from the emulsions in the absence of US during the ACT measurements (Fig. 6). However, due to the high loading of thrombin within the emulsions (417 IU/mL), the release of a small amount of thrombin could alter the ACT (Figs. 4 and 6). This release could have been facilitated by the movement of the magnet over the glass beads in the ACT tube, thereby grinding the droplets. *In vitro* studies have indicated that less than 0.1 IU/mL thrombin is required to trigger the onset of clot formation, whereas the concentration of free thrombin during a coagulation reaction ranges from less than 0.1 IU/mL to greater than 11.5–57.5 IU/mL (66). Comparatively, the normal concentration of prothrombin (factor II), the inactive precursor of thrombin, is approximately 1.3 IU/mL in adult humans (67). As seen in Fig. 6 and Table II, T3 displayed the largest and smallest ACT values before and after ADV, respectively. Thrombin was most highly retained in T3 before ADV, whereas ADV caused a ten-fold increase in the amount of thrombin released (Table III). Due to larger mean diameter of T3 (27.4 μm) relative to the other thrombin formulations, T3 is most amenable to intraarterial administration, similar to double emulsions utilized in the treatment of hepatocellular carcinoma (68).

The effect of ADV on protein stability, specifically proteins released from PFC emulsions via ADV, is currently unknown. Previous work (42) demonstrated that ADV can occur independently of inertial cavitation, a mechanism that can induce molecular damage. The volume percent of droplets vaporized (Table II) was larger than the percent of thrombin released estimated using the concentrations in Table III. For example, 28.7% (by volume) of T4 was vaporized as a result of ADV, but only 2.4% of the thrombin was released based on the measured ACT. As seen in Fig. 4, the ACT levels off for thrombin concentrations higher than 10 IU/mL; thus, the ACT cannot be used to calculate high thrombin concentrations, such as that which would be obtained theoretically if complete thrombin release from the emulsion were to occur (46.3 IU/mL). Even with this consideration, the large difference between the volume percent of droplets vaporized and the percent of thrombin released could indicate that ADV is inactivating the thrombin, especially considering the rapid consumption of PFC observed during ADV (43). Precipitated thrombin—an indicator of thrombin inactivation—was not seen with T3 after ADV, despite the complete vaporization of the emulsion; due to the partial vaporization of the other formulations, it was not possible to observe precipitated thrombin. Previous studies (17) focusing on the release of a small-molecular-weight compound (304.2 g/mol) via ADV did not demonstrate molecular inactivation due to ADV. Large molecules, such as thrombin (~36,000 g/mol), can experience broken chemical bonds due to the shear forces generated by the rapid motion of solvent following cavitational collapse (69). Additionally, as seen for T2 (Fig. 6), ADV caused additional inactivation of thrombin that had already been partially inactivated, which causes the ACT to increase after droplet vaporization. The investigation of acoustic parameters that would maximize thrombin release but minimize the apparent thrombin inactivation is beyond the scope of this work.

CONCLUSIONS

PFC double emulsions can serve as carriers for water-soluble therapeutic agents. These emulsions can be vaporized using US, thereby releasing the encapsulated agent from the emulsions via ADV. The use of a Kytox-PEG copolymer, which was found to have antithrombotic properties at higher concentrations, enabled the stable formation of the primary emulsion. Both fluorescein and thrombin were highly retained in the emulsions; ADV caused a statistically significant increase in fluorescein and thrombin release. The results also suggest that thrombin inactivation may be occurring as a result of the ADV process. Future studies are focused on understanding this inactivation, especially as it relates to ADV and inertial cavitation, and demonstrating the synergisms of ADV and drug delivery *in vivo*.

ACKNOWLEDGMENTS

The authors would like to thank Dr. Xia Shao (Department of Nuclear Medicine, University of Michigan, Ann Arbor, MI) for assistance with the Krytox-PEG copolymer synthesis and Dr. Kim Ives (Department of Radiology, University of Michigan, Ann Arbor, MI) for assistance in acquiring blood. The authors would also like to thank Dr. Olivier Couture (Ondes et Images, Institut Langevin, Paris, France) for useful discussions regarding reverse PFC emulsions. This work was supported in part by NIH grant 5R01EB000281.

REFERENCES

1. Dayton PA, Zhao S, Bloch SH, Schumann P, Penrose K, Matsunaga TO, *et al.* Application of ultrasound to selectively localize nanodroplets for targeted imaging and therapy. Mol Imaging. 2006;5(3):160–74.
2. Ganta S, Devalapally H, Shahiwala A, Amiji M. A review of stimuli-responsive nanocarriers for drug and gene delivery. J Control Release. 2008;126(3):187–204.
3. Laing ST, Kim H, Kopechek JA, Parikh D, Huang S, Klegerman ME, *et al.* Ultrasound-mediated delivery of echogenic immunoliposomes to porcine vascular smooth muscle cells *in vivo*. J Liposome Res. 2010;20(2):160–7.

4. Rapoport N. Physical stimuli-responsive polymeric micelles for anti-cancer drug delivery. Prog Polym Sci. 2007;32(8):962–90.
5. Unger EC, Porter T, Culp W, LaBell R, Matsunaga T, Zutshi R. Therapeutic applications of lipid-coated microbubbles. Adv Drug Deliv Rev. 2004;56(9):1291–314.
6. Eisenbrey JR, Burnstein OM, Kambhamptai R, Forsberg F, Liu J, Wheatley M. Development and optimization of doxorubicin loaded poly(lactic acid) contrast agent for ultrasound directed drug delivery. J Control Release. 2010;143(1):38–44.
7. Lentacker I, Geers B, Demeester J, Smedt SCD, Sanders NN. Design and evaluation of doxorubicin-containing microbubbles for ultrasound-triggered doxorubucin delivery: cytotoxicity and mechanisms involved. Mol Ther. 2010;18(1):101–8.
8. Liang H, Tang J, Halliwell M. Sonoporation, drug delivery, and gene therapy. Proc Inst Mech Eng H. 2010;224(H2):343–61.
9. Ren JL, Xu CS, Zhou ZY, Zhang Y, Li XS, Zheng YY, *et al.* A novel ultrasound microbubble carrying gene and tat peptide: preparation and characterization. Acad Radiol. 2009;16 (12):1457–65.
10. Datta S, Coussios CC, Ammi AY, Mast TD, de Courten-Myers GM, Holland CK. Ultrasound-enhanced thrombolysis using Definity as a cavitation nucleation agent. Ultrasound Med Biol. 2008;34(9):1421–33.
11. Yang FY, Liu SH, Ho FM, Chang CH. Effect of ultrasound contrast agent dose on the disruption of focused-ultrasound-induced blood-brain barrier disruption. J Acoust Soc Am. 2009;126(6):3344–9.
12. Dayton PA, Ferrara KW. Targeted imaging using ultrasound. J Magn Reson Imaging. 2002;16(4):362–77.
13. Hernot S, Klibanov AL. Microbubbles in ultrasound-triggered drug and gene delivery. Adv Drug Deliv Rev. 2008;60(10):1153–66.
14. Tinkov S, Bekeredjian R, Winter G, Coester C. Microbubbles as ultrasound triggered drug carriers. J Pharm Sci. 2009;98(6):1935–61.
15. Diaz-Lopez R, Tsapis N, Fattal E. Liquid perfluorocarbons as contrast agents for ultrasonography and 19F-MRI. Pharm Res. 2010;27(1):1–16.
16. Riess JG. Oxygen carriers ("blood substitutes")—raison d'etre, chemistry, and some physiology. Chem Rev. 2001;101(9):2797–919.
17. Fabiilli ML, Haworth KJ, Sebastian IE, Kripfgans OD, Carson PL, Fowlkes JB. Delivery of chlorambucil using acoustically-triggered, perfluoropentane emulsions. Ultrasound Med Biol. 2010;36(8):1364–75.
18. Fang JY, Hung CF, Liao MH, Chien CC. A study of the formulation design of acoustically active lipospheres as carriers for drug delivery. Eur J Pharm Biopharm. 2007;67(1):67–75.
19. Fang JY, Hung CF, Hua SC, Hwang TL. Acoustically active pefluorocarbon nanoemulsions as drug delivery carriers for camptothecin: drug release and cytoxicity against cancer cells. Ultrasonics. 2009;49(1):39–46.
20. Hwang TL, Lin YJ, Chi CH, Huang TH, Fang JY. Development and evaluation of perfluorocarbon nanobubbles for apomorphine delivery. J Pharm Sci. 2009;98(10):3735–47.
21. Apfel RE. Activatable infusable dispersions containing drops of a superheated liquid for methods of therapy and diagnosis. Patent 5,840,276, Apfel Enterprises, Inc., November 1998.
22. Giesecke T, Hynynen K. Ultrasound-mediated cavitation thresholds of liquid perfluorocarbon droplets *in vitro*. Ultrasound Med Biol. 2003;29(9):1359–65.
23. Kripfgans OD, Fowlkes JB, Miller DL, Eldevik OP, Carson PL. Acoustic droplet vaporization for therapeutic and diagnostic applications. Ultrasound Med Biol. 2000;26(7):1177–89.
24. Kawabata K, Sugita N, Yoshikawa H, Azuma T, Umemura S. Nanoparticles with multiple perfluorocarbons for controllable ultrasonically induced phase shifting. Jpn J Appl Phys. 2005;44 (6B):4548–52.
25. Rapoport NY, Kennedy AM, Shea JE, Scaife CL, Nam KH. Controlled and targeted tumor chemotherapy by ultrasound-activated nanoemulsions/microbubbles. J Control Release. 2009;138(2):268–76.
26. Kripfgans OD, Fowlkes JB, Woydt M, Eldevik OP, Carson PL. *In vivo* droplet vaporization for occlusion therapy and phase aberration correction. IEEE Trans Ultrason Ferroelectr Freq Control. 2002;49(2):726–38.
27. Kripfgans OD, Orifici CM, Carson PL, Ives KA, Eldevik OP, Fowlkes JB. Acoustic droplet vaporization for temporal and spatial control of tissue occlusion: A kidney study. IEEE Trans Ultrason Ferroelectr Freq Control. 2005;52(7):1101–10.
28. Zhang M, Fabiilli ML, Haworth KJ, Fowlkes JB, Kripfgans OD, Roberts W, *et al.* Initial investigation of acoustic droplet vaporization for occlusion in canine kidney. Ultrasound Med Biol. 2010;36(10):1691–703.
29. Arima K, Yamakado K, Kinbara H, Nakatsuka A, Takeda K, Sugimura Y. Percutaneous radiofrequency ablation with transarterial embolization is useful for treatment of stage 1 renal cell carcinoma with surgical risk: results at 2-year mean follow up. Int J Urol. 2007;14(7):585–90.
30. Wu F, Wang Z, Chen W, Zou J, Bai J, Zhu H, *et al.* Advanced hepatocellular carcinoma: treatment with high-intensity focused ultrasound ablation combined with transcatheter arterial embolization. Radiology. 2005;235(2):659–67.
31. Charbonnet P, Toman J, Buhler L, Vermeulen B, Morel P, Becker C, *et al.* Treatment of gastrointestinal hemorrhage. Abdom Imaging. 2005;30(6):719–26.
32. Petroianu A. Arterial embolization for hemorrhage caused by hepatic arterial injury. Dig Dis Sci. 2007;52(10):2478–81.
33. Debrun G, Aletich V, Ausman J, Charbel F, Dujovny M. Embolization of the nidus of brain arteriovenous malformations with n-butyl cyanoacrylate. Neurosurgery. 1997;40(1):112–20.
34. Taki W, Yonekawa Y, Iwata H, Uno A, Yamashita K, Amemiya H. A new liquid material for embolization of arteriovenous-malformations. AMJR Am J Neuroradiol. 1990;11(1):163–8.
35. Yamashita K, Taki W, Iwata H, Kikuchi H. A cationic polymer, Eudragit-E as a new liquid embolic material for arteriovenous malformations. Neuroradiology. 1996;38 Suppl 1:S151–6.
36. Krueger K, Zaehringer M, Strohe D, Struetzer H, Boecker J, Lackner K. Postcatheterization pseudoaneurysm: results of US-guided percutaneous thrombin injection in 240 patients. Radiology. 2005;236(3):1104–10.
37. Paulson EK, Sheafor DH, Kliewer MA, Nelson RC, Eisenberg LB, Sebastian MW, *et al.* Treatment of iatrogenic femoral arterial pseudoaneurysms: comparison of US-guided thrombin injection with compression repair. Radiology. 2000;215(2):403–8.
38. Holtze C, Rowat AC, Aggresti JJ, Hutchinson JB, Angile FE, Schmitz CHJ, *et al.* Biocompatible surfactants for water-in-fluorocarbon emulsions. Lab Chip. 2008;8(10):1632–9.
39. Tonelli C, Di Meo A, Fontana S, Russo A. Perfluoropolyether functional oligomers: unusual reactivity in organic chemistry. J Fluor Chem. 2002;118(1–2):107–21.
40. Zhu S, Edmonds WF, Hillmyer MA, Lodge TP. Synthesis and self-assembly of highly incompatible polybutadiene-poly(hexafluoropropylene oxide) diblock copolymers. J Polym Sci B Polym Phys. 2005;43(24):3685–94.
41. Benichou A, Aserin A. Recent developments in O/W/O multiple emulsions. In: Aserin A, editor. Multiple emulsions: technology and applications. Hoboken: Wiley-Interscience; 2008. p. 165–207.
42. Fabiilli ML, Haworth KJ, Fakhri NH, Kripfgans OD, Carson PL, Fowlkes JB. The role of inertial cavitation in acoustic droplet vaporization. IEEE Trans Ultrason Ferroelectr Freq Control. 2009;56(5):1006–17.

43. Kripfgans OD, Fabiilli ML, Carson PL, Fowlkes JB. On the acoustic vaporization of micrometer-sized droplets. J Acoust Soc Am. 2004;116(1):272–81.
44. Gibson J, Rees S, McManus T, Scheitlin W. A citrate-phosphate-dextrose solution for the preservation of human blood. Am J Clin Pathol. 1957;28(6):569–78.
45. Edwards C, Heptinstall S, Lowe K. Pluronic F-68 inhibits agonist-induced platelet aggregation in whole human blood *in vitro*. Artif Cells Blood Substit Immobil Biotechnol. 1998;26(5):441–7.
46. Moghimi SM, Hunter AC. Poloxamers and poloxamines in nanoparticle engineering and experimental medicine. Trends Biotechnol. 2000;18(10):412–20.
47. Florence AT, Whitehill D. The formulation and stability of multiple emulsions. Int J Pharm. 1982;11(4):277–308.
48. Matsumoto S, Kita Y, Yonezawa D. An attempt at preparing water-in-oil-in-water multiple-phase emulsions. J Colloid Interface Sci. 1976;57(2):353–61.
49. Zhang X, Liu X, Gu D, Zhou W, Xie T, Mo Y. Rheological models for xanthan gum. J Food Eng. 1996;27(2):203–9.
50. Putney SD. Encapsulation of proteins for improved delivery. Curr Opin Chem Biol. 1998;2(4):548–52.
51. Le Borgne SL, Graber M. Amidase activity and thermal stability of human thrombin. Appl Biochem Biotechnol. 1994;48(2):125–35.
52. Papadopoulou MV, Ji M, Bloomer WD. NLCQ-1, a novel hypoxic cytotoxin: potentiation of melphalan, cisDDP and cyclophosphamide *in vivo*. Int J Radiat Oncol Biol Phys. 1998;42(4):775–9.
53. Courrier HM, Vandamme TF, Krafft MP. Reverse water-in-fluorocarbon emulsions and microemulsions obtained with a fluorinated surfactant. Colloids Surf A Physiochem Eng Asp. 2004;244(1–3):141–8.
54. Jeon S, Lee J, Andrade J, de Gennes P. Protein-surface interactions in the presence of polyethylene oxide. J Colloid Interface Sci. 1991;142(1):149–58.
55. Roach LS, Song H, Ismagilov RF. Controlling nonspecific protein adsorption in a plug-based microfluidic system by controlling interfacial chemistry using fluorous-phase surfactants. Anal Chem. 2005;77(3):785–96.
56. Clausell-Tormos J, Lieber D, Baret JC, El-Harrak A, Miller OJ, Frenz L, *et al.* Droplet- based microfluidic platforms for the encapsulation and screening of mammalian cells and multicellular organisms. Chem Biol. 2008;51(42):427–37.
57. Jumaa M, Muller BW. The effect of oil components and homogenization conditions on the physiochemical properties and stability of parenteral fat emulsions. Int J Pharm. 1998;163(1):81–9.
58. Lundblad RL, Bradshaw RA, Gabriel D, Ortel TL, Lawson J, Mann KG. A review of the therapeutic uses of thrombin. Thromb Haemost. 2004;91(5):851–60.
59. Jesty S. The kinetics of inhibition of α-thrombin in human plasma. J Biol Chem. 1986;261(22):10313–8.
60. Chandy T, Das GS, Wilson RF, Rao GH. Development of polylactide microspheres for protein encapsulation and delivery. J Appl Polym Sci Symp. 2002;86(5):1285–95.
61. Ziv O, Lublin-Tennenbaum T, Margel S. Synthesis and characterization of thrombin conjugated γ-Fe_2O_3 magnetic nanoparticles for hemostasis. Adv Eng Mat. 2009;11(12):B251–60.
62. Ziv-Polat O, Topaz M, Brosh T, Margel S. Enhancement of incisional wound healing by thrombin conjugated iron oxide nanoparticles. Biomaterials. 2010;31(4):741–7.
63. Marchioni C, Riccardi E, Spinelli S, dell'Unto F, Grimaldi P, Bedini A, *et al.* Structural changes induced in proteins by therapeutic ultrasounds. Ultrasonics. 2009;49(6–7):569–76.
64. Oliva A, Santovena A, Farina J, Llabres M. Effect of high shear rate on stability of proteins: kinetic study. J Pharm Biomed Anal. 2003;33(2):145–55.
65. Jiao J, Burgess DJ. Multiple emulsion stability: pressure balance and interfacial film strength. In: Aserin A, editor. Multiple emulsions: technology and applications. Hoboken: Wiley-Interscience; 2008. p. 1–28.
66. Wolberg AS. Thrombin generation and fibrin clot structure. Blood Rev. 2007;21(3):131–42.
67. Andrew M, Paes B, Milner R, Johnston M, Mitchell L, Tollefsen DM, *et al.* Development of the human coagulation system in the full-term infant. Blood. 1987;70(1):165–72.
68. Higashi S, Tabata N, Kono K, Maeda Y, Shimizu M, Nakashima T, *et al.* Size of lipid microdroplets effects results of hepatic arterial chemotherapy with an anticancer agent in water-in-oil-in-water emulsion to hepatocellular carcinoma. J Pharmacol Exp Ther. 1999;289(2):816–9.
69. Taghizadeh M, Asadpour T. Effect of molecular weight on the ultrasonic degradation of poly(vinyl-pyrrolidone). Ultrason Sonochem. 2009;16(2):280–6.